Geothermics 46 (2013) 22–31

Contents lists available at SciVerse ScienceDirect

Geothermics

journal homepage: www.elsevier.com/locate/geothermics

Analytical approach to groundwater-influenced thermal response tests of grouted borehole heat exchangers

Valentin Wagner[a,*], Philipp Blum[a], Markus Kübert[b], Peter Bayer[c]

[a] Karlsruhe Institute of Technology (KIT), Institute for Applied Geosciences (AGW), Kaiserstraße 12, 76131 Karlsruhe, Germany
[b] tewag Technologie – Erdwärmeanlagen – Umweltschutz GmbH, Am Haag 12, 72181 Starzach-Felldorf, Germany
[c] ETH Zurich, Engineering Geology, Sonneggstrasse 5, 8092 Zurich, Switzerland

ARTICLE INFO

Article history:
Received 17 October 2011
Accepted 26 October 2012

Keywords:
Geothermal energy
Thermal response test
Groundwater velocity
Thermal conductivity
Thermal borehole resistance

ABSTRACT

For ground-source heat pump (GSHP) systems, the thermal response test (TRT) is commonly used to determine the heat transport parameters of the subsurface. The main limitation of this approach is the assumption of pure conductive heat transport, which might result in significant deviations. Based on the moving line source theory, a parameter estimation approach is introduced, which is sensitive to conduction and advection. This approach is calibrated and successfully tested against three different test cases. The presented analytical approach therefore expands the field of application of the TRT to advection-influenced conditions beyond a Darcy velocity of 0.1 m day^{-1}.

1. Introduction

The heat stored in the shallow subsurface is of growing interest to geothermal energy use. In the upper hundreds of meters of the earth's crust, the temperature usually does not reach much more than 20 °C (e.g., Taniguchi and Uemura, 2005; Zhu et al., 2011). Thus, the energy is only useful for space heating and air conditioning systems and is ideally extracted from wells or boreholes (in general to a depth of around 150 m (e.g., Hecht-Méndez et al., 2010)) combined with heat pumps. Alternatively, the ground may be used as storage medium for waste heat or for cooling purposes (Sanner et al., 2003). The most common variants of geothermal systems are ground-source heat pumps (GSHPs), where vertical boreholes act as borehole heat exchangers (BHEs) (Rybach and Eugster, 2010). A heat carrier fluid is circulated in closed tubes installed in the boreholes. In the heating mode, the injection temperature is slightly lower than the temperature of the ground. Circulation in the subsurface warms up the fluid and by operating the heat pump, the collected energy is extracted above, thus cooling the ambient ground. Temperature anomalies develop, and the radial temperature gradient forces the heat flow toward the BHE.

Since the geological, geophysical, and hydrogeological conditions that control the heat transfer processes and extraction efficiency vary, field investigation campaigns are suggested for larger-scale systems to ensure appropriate planning of shallow geothermal installation. The thermal response test (TRT), which is conducted in BHEs before heat mining begins is an established technique (Morgensen, 1983; Gehlin, 2002; Sanner et al., 2005; Signorelli et al., 2007; Beier et al., 2011; Raymond et al., 2011a,c). By monitoring the effect of short-term heating (or cooling), the thermal properties of the ground and the heat transfer efficiency between ground and BHE are interpreted.

In standard experiments, a heated or cooled fluid is injected and the temperature development, i.e. the response of the ground, is monitored at the BHE outlet. The slower the temperatures of the heat carrier fluid increase, the more heat is lost in the ground and, thus, the higher is the interpreted in situ effective thermal conductivity. The temperature time series are commonly evaluated based on the Kelvin line source theory that assumes an infinite, homogeneous and isotropic medium with a constant heat source (Carslaw and Jaeger, 1959). This evaluation provides the effective thermal conductivity (λ_{eff}) as well as the thermal borehole resistance (R_b), which is a measure of the heat transfer performance in the borehole. Both parameters are used for a case-specific planning and efficient operation of the GSHP system.

Standard TRT interpretation exhibits several shortcomings. It assumes a homogenous subsurface, no axial heat transport, uniform initial temperature distribution, and it approximates the BHE shape as an infinite line. Bandos et al. (2009) presented an analytical solution to overcome the limitations caused by the assumption of an infinite line shape. Another significant shortcoming is that only conductive heat transport is considered (e.g., Signorelli et al., 2007). However, shallow geothermal systems are

* Corresponding author. Tel.: +49 721 608 45065; fax: +49 721 606 279.
E-mail address: valentin.wagner@kit.edu (V. Wagner).

0375-6505/$ – see front matter © 2012 Elsevier Ltd. All rights reserved.
http://dx.doi.org/10.1016/j.geothermics.2012.10.005

Nomenclature

C	correction factor
c_p	volumetric heat capacity (MJ m^{-3} K^{-1})
D	thermal dispersion coefficient (m^2 s^{-1})
d_s	shank spacing (m)
Ei	exponential integral
k	hydraulic conductivity (m s^{-1})
Pe	Péclet number
q	heat transfer rate per unit length (W m^{-1})
r	radius (m)
r_{pin}	inner pipe radius (m)
r_{pout}	outer pipe radius (m)
R_b	thermal borehole resistance (m K W^{-1})
T	temperature (°C)
t	time (s)
t_c	time criterion (s)
u	integration variable
v	Darcy velocity (m day^{-1})
v_{th}	heat transport velocity (m day^{-1})
x, y	Cartesian coordinates (m)

Greek symbols

α	dispersivity (m)
λ	thermal conductivity (W m^{-1} K^{-1})
κ	thermal diffusivity (m^2 s^{-1})
γ	Euler constant

Subscripts and superscripts

f	heat carrier fluid
bw	borehole wall
sub	property of the subsurface
g	property of the grouting material
eff	obtained effective property value (without correction)
m	property of the porous medium
w	property of the groundwater
0	initial or undisturbed value
l	longitudinal
t	transversal
*	value corrected by C

frequently installed in water-saturated undergrounds. In aquifers, advective heat transfer due to groundwater flow can be significant (e.g., Witte, 2001). Accordingly, the effective thermal conductivity (λ_{eff}) obtained based on the Kelvin line source theory is an apparent parameter, which increases with Darcy velocity. Several studies have demonstrated the significant influence of groundwater flow (Witte and Gelder, 2006) and ambient air temperature variations (Bandos et al., 2011) on TRT results. Witte (2001) established an advection-dominated aquifer by performing a TRT, while groundwater was being extracted from a well 5 m away from the BHE. A comparison to the results of an undisturbed TRT showed an increase in the λ_{eff} value by a factor of 1.38. This relationship was also investigated by Bozdag et al. (2008), who performed four different TRTs in one BHE and correlated the obtained λ_{eff} and R_b values with the observed different hydraulic gradients. Their field measurements clearly indicated the influence of water table fluctuations, which govern groundwater flow velocities, on the TRT results. The influence of groundwater flow is also examined by several theoretical studies. For instance, Chiasson et al. (2000) numerically simulated TRTs to analyze the role of groundwater flow velocity and different evaluation periods with respect to the value of λ_{eff} that would be obtained by the line-source approach. They demonstrated that the resulting thermal conductivity value is an effective one and does not represent the thermal conductivity of the subsurface. Signorelli et al. (2007) comprehensively analyzed those effects and confirmed the findings by Witte (2001) that λ_{eff} increases continuously with evaluation time. In essence, the line source-based TRT evaluation of advection-dominated systems results in ambiguous λ_{eff} values. Signorelli et al. (2007) conclude that BHE dimensioning based on λ_{eff} in advection-dominated systems is rather problematic, because of the increasing instability of the resulting values.

A number of remedies have been suggested to reliably evaluate TRTs influenced by groundwater flow. One possibility to detect the influence of groundwater flow is a stepwise TRT evaluation based on the Kelvin line source theory (e.g., Sanner et al., 2005). Witte (2001) interpreted an increasing λ_{eff} value with increasing evaluation time step size as an indicator for groundwater flow. Another possibility is an enhanced TRT (Wagner and Rohner, 2008), where depth-depending temperature series during and/or after the heating period are evaluated (Fujii et al., 2009). Wagner and Rohner (2008) showed how specific layers with groundwater flow (enhanced λ_{eff} values) can be estimated. However, these concepts provide no information about the actual Darcy velocity. To overcome this, parameter estimation approaches based on numerical simulations (Raymond et al., 2011b) or alternative analytical equations (Katsura et al., 2006) were suggested. Raymond et al. (2011b) numerically quantified that the TRT examined at a field site was influenced by a groundwater flow velocity smaller than 10^{-5} m s^{-1}. Based on several simulation results with a groundwater flux between 10^{-6} and 10^{-8} m s^{-1} and λ_m values between 2.35 and 2.65 W m^{-1} K^{-1}, the measured temperature values could be reproduced (Raymond et al., 2011b). In a different context, Katsura et al. (2006) analyzed the heat response of a thermal probe in a sand-filled cylinder influenced by different water flow velocities. By calibration of the moving line source equation (Carslaw and Jaeger, 1959) to the measured thermal response it was possible to derive the groundwater velocity with a relative error of less than 20% (Katsura et al., 2006).

Previous studies have demonstrated the ambiguous character of the parameters determined by line source-based TRT evaluation, especially if groundwater flow influences the system. The objective of this study is therefore to develop an analytical approach to groundwater-influenced TRTs, which provides parameters more suitable for a detailed simulation of conductive and advective heat transport in the subsurface. For this purpose, an approach in line with the one by Katsura et al. (2006) is developed. Furthermore, we introduce a correction term to consider the effects caused by the lower hydraulic conductivity of a grouted BHE on the apparent (i.e., estimated) Darcy velocity in the vicinity of the BHE. This correction term is calibrated by artificially generated high-resolution TRT temperature time series and embedded in a parameter estimation framework. Finally, the applicability of this concept for the simultaneous determination of ground thermal conductivity, λ_m, and Darcy velocity, v, is discussed based on a set of scenarios adopted from related studies.

2. TRT models

2.1. Conductive line source

The most widely used procedure to evaluate a TRT is based on the Kelvin line source theory. This approach approximates the BHE as an infinite line source in a homogeneous, isotropic and infinite medium, which injects or extracts a constant amount of energy (q) by conductive heat transport only. The temporal and spatial temperature changes around the line source can be calculated as

follows (e.g. Carslaw and Jaeger, 1959; Gehlin, 2002; Signorelli et al., 2007):

$$T_{sub}(r,t) - T_0 = \frac{q}{4\pi\lambda_{eff}} \int_{r^2/4\kappa t}^{\infty} \frac{e^{-u}}{u} du = \frac{q}{4\pi\lambda_{eff}} E_i\left[\frac{r^2}{4\kappa t}\right] \approx \frac{q}{4\pi\lambda_{eff}}\left[\ln\left(\frac{4\kappa t}{r^2}\right) - \gamma\right] \quad (1)$$

The maximum error of the logarithmic approximation of the exponential integral is less than 10%, if the time criterion $t \geq t_c \geq 5\, r_{bw}^2\, \kappa^{-1}$ is fulfilled (Hellström, 1991). This error range assumes that substantial disturbances on the recorded temperatures are absent and the test is properly executed. To be able to calculate the mean fluid temperature, the thermal resistance R_b between the borehole wall and the circulating heat carrier fluid has to be considered. This leads to the following extension of Eq. (1):

$$T_f - T_{bw} = q \cdot R_b \quad (2)$$

$$T_f(t) = T_{bw}(t) + qR_b = \frac{q}{4\pi\lambda_{eff}} E_i\left[\frac{r_{bw}^2}{4\kappa t}\right] + T_0 + R_b q \approx \frac{q}{4\pi\lambda_{eff}} \ln(t) + q\left[R_b + \frac{1}{4\pi\lambda_{eff}}\left(\ln\left(\frac{4\kappa t}{r_{bw}^2}\right) - \gamma\right)\right] + T_0 \quad (3)$$

To determine the effective thermal properties (λ_{eff} and R_b), two similar approaches are possible. The recorded TRT data are either fitted by a two-variable parameter estimation technique (Roth et al., 2004) or by a linear regression based on the logarithmic approximation of Eq. (3) (Gehlin, 2002; Signorelli et al., 2007). A TRT evaluation based on the Kelvin line source theory does not consider the effects of groundwater flow and simplifies all possible heat transfer processes of the subsurface as purely conductive transport with an effective thermal conductivity, λ_{eff}. Therefore, it is not possible to determine the relevant heat transport parameters for advection-dominated conditions using Eq. (3).

2.2. Moving line source

To determine adequate parameters for the simultaneous heat transport by advection and conduction, another analytical equation is necessary. Carslaw and Jaeger (1959) derived a suitable analytical equation, which simulates a constant line source of infinite length in a homogeneous and infinite medium and in its extended version additionally accounts for advection and hydrodynamic dispersion (Metzger et al., 2004; Molina-Giraldo et al., 2011). The temperature difference caused by the line source is calculated by:

$$T_{sub}(x,y,t) - T_0 = \frac{q}{4\pi c_{pm}\sqrt{D_l D_t}} \exp\left[\frac{v_{th}x}{2D_l}\right] \times \int_0^{v_{th}^2 t/4D_l} \exp\left[-\left(\frac{x^2}{D_l} + \frac{y^2}{D_t}\right)\frac{v_{th}^2}{16D_l u} - u\right]\frac{du}{u} \quad (4)$$

Equivalent to the approach by Sutton et al. (2002), the fluid temperature of a BHE can be accessed by adding a thermal borehole resistance term. Eq. (4) is extended as follows if the Cartesian coordinates fulfill the condition $x^2 + y^2 = r_{bw}^2$:

$$T_f(x,y,t) = \frac{q}{4\pi c_{pm}\sqrt{D_l D_t}} \exp\left[\frac{v_{th}x}{2D_l}\right] \int_0^{v_{th}^2 t/4D_l} \exp\left[-\left(\frac{x^2}{D_l} + \frac{y^2}{D_t}\right)\frac{v_{th}^2}{16D_l u} - u\right]\frac{du}{u} + T_0 + R_b q \quad (5)$$

Eqs. (4) and (5) account for an effective heat transport velocity (v_{th}) and an effective thermal dispersion coefficient (D_l and D_t). These parameters are determined as follows:

$$v_{th} = v_{eff}\frac{c_{pw}}{c_{pm}} \quad (6)$$

$$D_l = \frac{\lambda_{m,\,eff}}{c_{pm}} + \alpha_l v_{th} \quad (7)$$

$$D_t = \frac{\lambda_{m,\,eff}}{c_{pm}} + \alpha_t v_{th} \quad (8)$$

In contrast to λ_{eff}, $\lambda_{m,eff}$ in fact is an obtained value, but only represents the properties of the porous medium and contains no advective portion.

Eq. (5) additionally accounts for advective heat transport, but it still carries some simplifying assumptions. Similar to Eq. (2) for standard TRT interpretation, the effects of thermal disturbance, such as from vertical heat flow along the natural vertical geothermal gradient, are neglected. However, Wagner et al. (2012) demonstrated that this only introduces a minor error in standard TRT interpretation. Disturbances from buoyancy effect are also ignored. Hecht-Méndez et al. (2010) demonstrated this as a valid assumption for the simulation of common GSHP systems. Furthermore, Gehlin et al. (2003) reported that the thermosiphon effect, which is caused by a vertical groundwater flow inside the borehole, can be neglected for properly grouted BHE. It is important to emphasize that our TRT interpretation only provides subsurface properties averaged over the total length of the BHE. Both Eqs. (3) and (5) yield integral parameter sets to characterize the subsurface, and are not suited for resolving heterogeneous properties of the ground. Eq. (5) also assumes advective heat transport in a porous media, and the application to fractured rocks is restricted. For the latter, the evaluation by Gehlin et al. (2003) is therefore recommended.

We suggest a parameter estimation approach that calibrates Eq. (5) to temperature time series of a TRT, which uses the Nelder–Mead algorithm as explained for example by Lagarias et al. (1998). This minimizes the root mean squared error (RMSE) between observed (in this study: the numerically generated dataset) and calculated data (Eq. (5)) by varying a defined set of functional parameters. The RMSE determines the accuracy of the fitting, and thus can be utilized to compare different calibration results. In general, when calibrating models to measurements in natural systems, the complex coupled processes involved often make it impossible that one unique set of valid model parameter values can be determined. For a given tolerance on the RMSE of the calibrated model it is thus suggested to estimate possible parameter ranges and, if they exist, to also extract correlations among different parameters (Maier et al., 2009). This insight is in particular valuable for ill-posed problems like the TRT evaluation based on Eq. (5), where solutions to the inverse problem are non-unique. For the estimation of $\lambda_{m,eff}$ and v_{eff} this is considered by setting a threshold on the RMSE equivalent to the expected measurement error of 0.1 °C, which Witte et al. (2002) mentioned as the accuracy of a temperature sensor. In reality, the measurement error might be different, because of the applied type of sensor, the kind of combination of temperature sensors and/or the temperature dependency of the sensor itself. To inspect whether acceptable locally optimal or close-optimal solutions to the error function exist, multiple randomly initialized Nelder–Mead-based minimization runs (here: 15) are applied. In this way, we gather sufficient sets of $\lambda_{m,eff}$ and v_{eff} pairs.

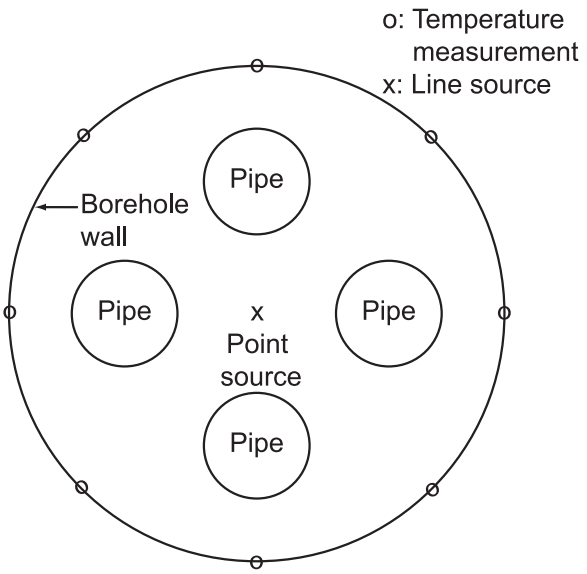

Fig. 1. Cross section of a BHE with central evaluation position of the line source equation and the temperature measurement locations at the borehole wall for calculation of mean temperature in the case of groundwater flow.

Eq. (5) is not suitable for TRT interpretation with a real BHE, since it does not explain the complex heat transfer inside the BHE. This was not relevant in the study by Katsura et al. (2006), who suggested the moving line source equation to evaluate the temperature difference in a sand-filled cylinder caused by a needle-shaped heating device in a laboratory experiment. In our approach, similar to that by Katsura et al. (2006), the effects of mechanical thermal dispersion are neglected in Eq. (5) in a first step. This is considered an acceptable simplification that reduces the number of unknown parameters. More details on potential errors introduced by this simplification are comprehensively discussed by Molina-Giraldo et al. (2011) and Wagner et al. (2012).

The second step computes a single representative borehole wall temperature, which is necessary for application of Eq. (5). The representative borehole wall temperature here is an integral value of the entire BHE. In contrast to a conduction-dominated system, the heat propagation in an advection-dominated system is not radially symmetric. Consequently, temperatures at the borehole wall are not constant. To account for the asymmetric heat distribution around a BHE influenced by groundwater flow, we calculate a mean borehole wall temperature measured at eight positions. These positions are predefined on the BHE cross section and depicted in Fig. 1.

The amount of energy transported by conduction and advection can be compared by the Péclet number *Pe* (Domenico and Palciauskas, 1973). Barcenilla et al. (2005) suggested the following formulation to calculate the Péclet number, *Pe*, of a BHE:

$$Pe = \frac{v r_{bw}}{\kappa} = \frac{v r_{bw} c_{pm}}{\lambda_m} \quad (9)$$

2.3. Two-dimensional finite element model for TRT simulation

The applicability of the moving line source equation (Eq. (5)) to evaluate the thermal response of a BHE is tested by comparing analytical to realistic numerical simulation. For this, a two-dimensional (2D) high-resolution finite element model in FEFLOW 5.4 (Diersch, 2006) is developed. The latter is developed by comparison to a more comprehensive 3D finite element model presented by Wagner et al. (2012). It is able to predict the complex heat transfer between the several parts of the BHE (heat carrier fluid, pipe wall and grout material), the porous medium, and the moving groundwater. In contrast, Eq. (5) considers the entire system as a line-shaped heat source in a homogeneous medium. Errors caused by this simplification can be evaluated by comparison between the numerical simulation and the results of Eq. (5). The numerical model specifications of simulated BHE geometry are listed in Table 1 and shown in Fig. 2, and the assumed material properties are provided in Table 2.

Table 1
Geometric settings of simulated borehole heat exchanger (BHE) in the numerical model (Fig. 2).

	Value
Radius of the borehole, r_{bw} (m)	0.075
Inner radius of the pipe, r_{pin} (m)	0.013
Outer radius of the pipe, r_{pout} (m)	0.016
Shank spacing, d_s (m)	0.093

Implementation of the BHE and the surrounding aquifer in the numerical grid is illustrated in Fig. 2. The discretization is refined for the parts with the highest expected gradients. This is the BHE itself and the downgradient eastern part of the subsurface, where the temperature plume evolves. Groundwater flow is simulated by a 2nd type boundary condition (BC) at the western and eastern boundary of the model, which assigns a constant flux (Diersch, 2006). The temperature of the inflowing groundwater is controlled by a 1st type BC, which assigns a constant temperature value to certain nodes. The temperature value is equal to the initial temperature of the entire system. The heat is injected in the surplus of the pipes by a 4th type BC, which defines cell-specific energy extraction/injection per time. The turbulent heat propagation inside the pipe is simulated by an enhanced thermal conductivity of the pipe surplus (Diersch et al., 2010).

3. Initial evaluation

3.1. Thermal borehole resistance

In an initial evaluation, the numerical model is employed to examine the influence of hydraulic parameters on the calculated

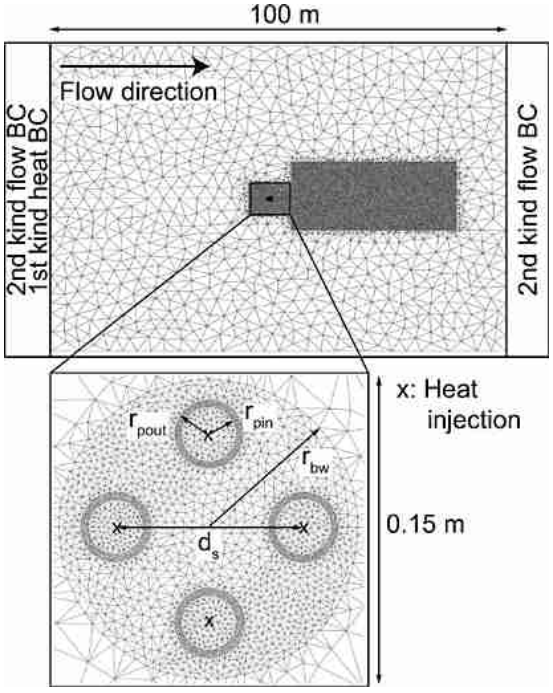

Fig. 2. Overview of model domain, spatial discretization, boundary conditions (BC), and parameters to characterize the simulated borehole heat exchanger (BHE). The shape of the BHE is defined by shank spacing d_s, borehole radius r_{bw}, outer pipe radius r_{pout}, and inner pipe radius r_{pin}.

Table 2
Hydraulic and thermal properties of different numerical model compartments.

Property	Hydraulic conductivity, k ($m\,s^{-1}$)	Thermal conductivity of porous medium, λ_m ($W\,m^{-1}\,K^{-1}$)	Volumetric heat capacity of porous medium, c_{pm} ($MJ\,m^{-3}\,K^{-1}$)
Subsurface	1.5×10^{-3} [a] (Hähnlein et al., 2010)	2.1[a] (Palmer et al., 1992)	2.8[a] (Palmer et al., 1992)
Grout material	6×10^{-8} [a] (Herrmann, 2008)	0.8[a] (Herrmann, 2008)	2.3[b] (Niekamp et al., 1984; Gauthier et al., 1997)
Pipe material	1×10^{-19} [c] (Pannike et al., 2006)	0.39[b] (Signorelli et al., 2007)	1.6[a] (Signorelli et al., 2007)
Heat carrier fluid (surplus)	1×10^{-19} [c] (Pannike et al., 2006)	≥20.0[b] (Clausen, 2008)	4.2[a] (Diersch et al., 2010)

[a] Reported realistic values.
[b] Estimated based on real values.
[c] Estimated to be able to run the model and avoid hydraulic interactions between the discrete feature elements and the part of the finite element mesh representing the grouting material and the subsurface.

borehole resistance, R_b, of a completely grouted BHE. Conditions in ungrouted and groundwater filled BHE might be different, reflected by a more transient behavior inside the BHE (e.g. Gustafsson and Gehlin, 2008; Gustafsson and Westerlund, 2010, 2011). The latter is calculated based on Eq. (2) and the simulated temperature values of the borehole wall, T_{bw}, and of the fluid, T_f. The borehole wall temperature T_{bw} is the arithmetic mean of temperature values which are obtained from nodes located at the boundary between the subsurface and the grout material. The position of the nodes applied to obtain the latter temperature values are specified in Fig. 1. The mean heat carrier fluid temperature, which is evaluated by the TRT approach, is the average temperature determined at the center nodes of each pipe (Fig. 2).

Using the numerical model, it is possible to quantify R_b for every simulation time step (Fig. 3). All thermal settings remain unchanged. The BHE is simulated with variable Darcy velocities, v, in the aquifer and two different hydraulic conductivities, k_g, of the grout material (Fig. 3). The first case analyzes R_b with respect to increasing v. In order to prevent the BHE from acting as hydraulic resistor, the hydraulic conductivity of the grouting material is set equal to the hydraulic conductivity of the subsurface ($k_g = k_{sub}$). Thus, groundwater flow penetrates the BHE, and conductive and advective heat transports inside the BHE occur. The additional advective component promotes heat transfer inside the BHE and therefore thermal borehole resistance, R_b, decreases with increasing Darcy velocity, v. If significant amounts of groundwater penetrate the grouted part of a BHE, adverse impacts on the grouting material might also occur.

The second case considers the more realistic hydraulic conductivity k_g contrast between grout and aquifer ($k_g \ll k_{sub}$). Herrmann (2008) measured hydraulic conductivity values of several grout materials, and accordingly a typical value of $k_g = 6 \times 10^{-8}\,m\,s^{-1}$ is selected here. Under such conditions, groundwater flows mainly around the BHE. The heat transfer inside the grout is considered purely conductive and only in the aquifer heat is transported by both conduction and advection. As a consequence, the calculated R_b values are nearly independent of the Darcy velocity (Fig. 3). The determined R_b time series of the second case shows small variations of the R_b values at the early time steps. The promoting effect of groundwater flow on the heat transport in the subsurface decreases the period of time to reach thermal steady-state conditions of the entire system (subsurface and BHE). To verify the obtained results, R_b values with an identical BHE setup are calculated based on the steady-state multipole method, which is implemented in the software Earth Energy Designer – EED (Hellström and Sanner, 2000). For all cases with a negligible advective heat transport inside the BHE, both approaches result in comparable values (discrepancy below 0.5%) for the time interval of 20–70 h. This time interval is also applied for subsequent TRT interpretations.

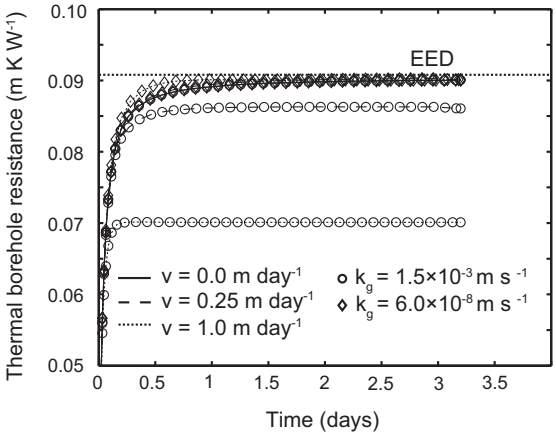

Fig. 3. Temporal sequence of thermal borehole resistance calculated from the numerical simulation result for different Darcy velocities, v, and hydraulic conductivity values, k_g, of the grouting material. The obtained results are compared to simulation by EED.

There are several similar methods available to determine R_b (e.g. Lamarche et al., 2010; Bauer et al., 2011), if the specifications of the BHE are known, like hydraulic and thermal properties of the grout material, U-tube spacing, borehole diameter. Chiasson and O'Connell (2011) demonstrated a good agreement of R_b values calculated by the multipole method and a moving line source parameter estimation approach. This means that in principle, no TRT is necessary to estimate this parameter, which is also assumed in the current study. Hence, the borehole resistance can be excluded from the evaluation of a TRT. Instead, it is predetermined as a case-specific constant, and the only unknowns, therefore, are v and λ_m. This facilitates the parameter estimation procedure, which is already difficult for standard TRT interpretation. The inversion problem revealed to be ill-posed in the studies by Marcotte and Pasquier (2008) and Wagner et al. (2012), which showed multiple λ_{eff} and R_b pairs yielding valid solutions. Accordingly, we also assess the determinability of TRT parameters in our proposed analytical approach for groundwater-influenced TRT.

3.2. TRT evaluation with moving line source

Several numerically generated TRT temperature time series are generated to analyze the suitability of the moving line source equation, Eq. (5), for determination of the Darcy velocity. Since a BHE is made up of different materials with specific property values, this violates the assumption of a homogeneous medium in Eq. (5). Thus, fitting TRT data might potentially cause errors for the results. Thermal properties are less variable than hydraulic properties, and therefore interpretation of purely conductive systems with the standard line source equation is feasible. Signorelli et al. (2007) analyzed numerically generated TRTs and showed that the error caused by the thermal conductivity difference between the grouting material and the subsurface of $\Delta\lambda = 2.2\,W\,m^{-1}\,K^{-1}$ is less than 5%. The difference of the model in our study is even smaller

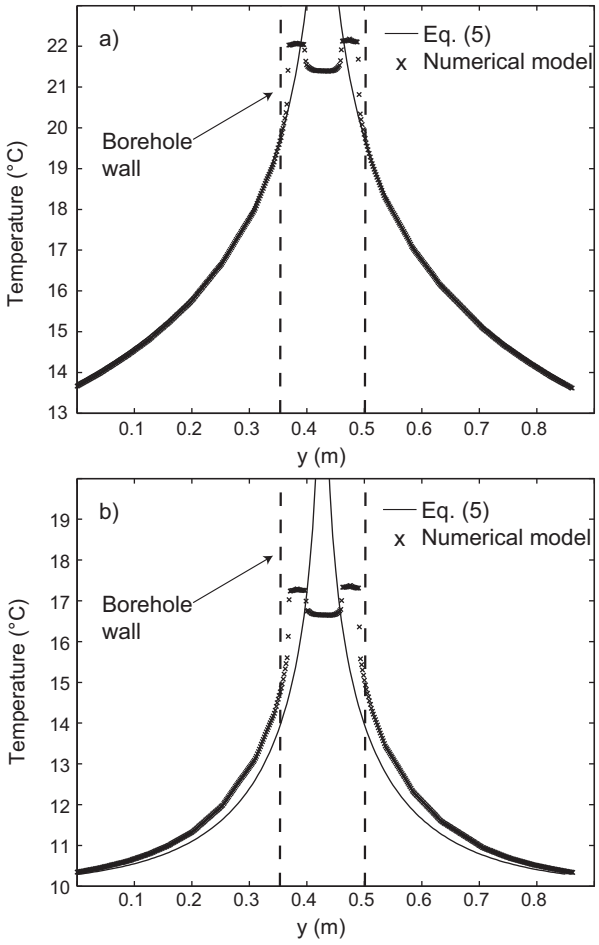

Fig. 4. Comparison of the spatial temperature distribution around a BHE perpendicular to the flow direction calculated using Eq. (5) and the numerical model presented in Section 2.3. (a) Temperature distribution for a pure conductive heat transfer around a BHE; (b) Temperature distribution for a conductive and advective heat transfer around a BHE (Darcy velocity: $v = 0.5\ \mathrm{m\,day^{-1}}$).

($\Delta\lambda = 1.3\ \mathrm{W\,m^{-1}\,K^{-1}}$, Table 2). This property contrast becomes even smaller when a thermally enhanced grout material is used to backfill the BHE, which is increasingly popular. The effect of this parameter difference is presented in Fig. 4a. The spatial temperature distribution calculated by Eq. (5) only deviates inside the BHE in comparison with the results of the numerical model. The heat transfer inside the BHE is approximated by the thermal borehole resistance; therefore, the temperature value at the borehole wall is relevant for TRT evaluation and, thus, the temperatures resulting at the borehole wall of the analytical solution and the numerical model are identical. Hence, we assume that the influence of the thermal conductivity contrast can be neglected.

The borehole resistance, R_b, should not be influenced by groundwater flow in the BHE-surrounding porous medium, and its value may be determined separately. Therefore, in the next analysis our focus is set exclusively on Darcy velocity, v, and thermal conductivity. Thermal borehole resistance values are fixed as given in Table 2. The question is, how well does the effective Darcy velocity (v_{eff}), determined by Eq. (5), approximate the known value of v specified in the numerical model? The results are based on repeated simulations of different hydraulic conditions, and parameter estimations with Eq. (5) and are illustrated in Fig. 5. According to Witte et al. (2002), all determined effective Darcy velocities are suitable with an RMSE smaller than the temperature measurement error of 0.1 °C. The average validity range of v_{eff} is smaller than ±2.5% of the optimal fit, which denotes that the moving line source delivers a

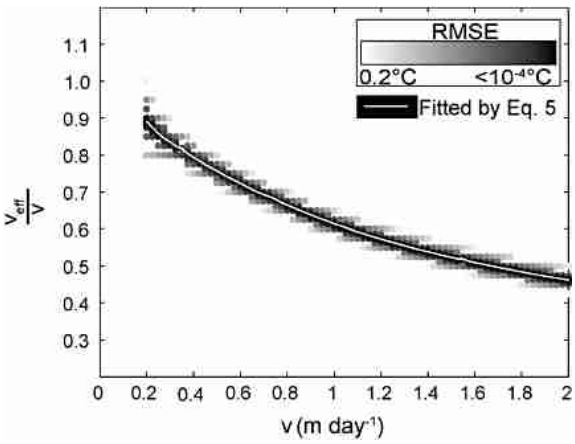

Fig. 5. Result of the evaluation of numerically generated TRT temperature time series (influenced by different Darcy velocities) based on the moving line source equation. Maximum tolerance of fitting error is set to an RMSE of 0.2 °C.

satisfactory result. The observed discrepancy between chosen v and best-fitted v_{eff} is unsatisfactory. The true value of Darcy velocity, v, is always underestimated, and the calculated conformance ratio even decreases non-linearly for higher groundwater velocities. For a high Darcy velocity of $v = 2\ \mathrm{m\,day^{-1}}$, for example, the best-fitted Darcy velocity is about 50% below the input value. For low values ($<0.2\ \mathrm{m\,day^{-1}}$), conduction dominates the heat transport and consequently the sensitivity of the advective component decreases. Under these conditions, the validity range of v_{eff} clearly exceeds ±2.5%, indicating that a small uncertainty in the thermal conductivity value causes significant relative errors of v_{eff} in this domain and a precise determination of the ratio v_{eff}/v is not possible.

This discrepancy between input and best-fitted Darcy velocity is mainly caused by the difference between the hydraulic conductivities of the grouting material and the aquifer. The latter (k_{sub}) applied in the current study is 2.5×10^4 times higher than that of the grouting material. Thus, the Darcy velocity is noticeably reduced in the close vicinity of the source, i.e. the BHE, which also explains why the best-fitted Darcy velocities are increasingly underestimated for increasing input velocities v. This effect is shown for the conduction and advection-influenced system in Fig. 4b. The determined temperature at the borehole wall calculated using Eq. (5) and the numerical model differ not only inside the BHE like in the case of conductive heat transfer, but also at the borehole wall. The deviation inside the BHE is reflected by the thermal borehole resistance R_b, but the discrepancy of T_{bw} values still remains. The latter hampers the application of Eq. (5), and instead only time-consuming numerical simulation appears to be suitable. However, as a systematic error is introduced by an evident process, a straightforward parametric approach is favored for practical applications. Hence, a correction term is included in the estimation procedure by Eq. (5), which is described in the subsequent section.

4. Correction

4.1. Correction term

A correction term, C, is introduced to balance the difference between v_{eff} and v:

$$v \approx v^*_{eff} = \frac{v_{eff}}{C} \tag{10}$$

For various hydraulic and thermal conditions, the ratio v_{eff}/v is calculated to obtain a robust specification of the correction term, which can be used to estimate a corrected Darcy velocity v^*_{eff}. Numerical simulations with a thermal conductivity range of the

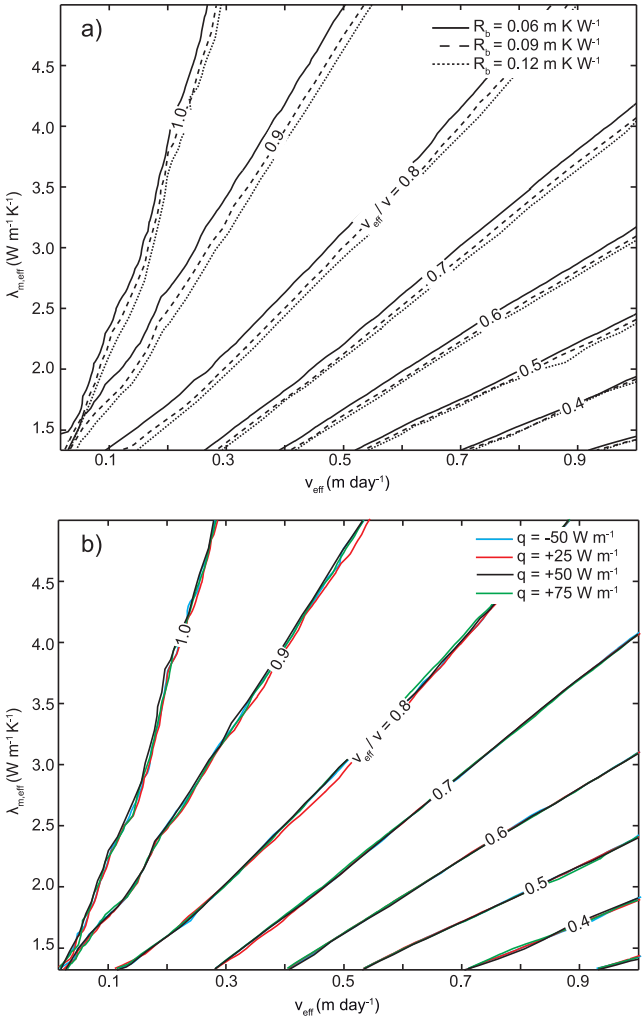

Fig. 6. Relation between the resulting parameters of the TRT evaluation based on Eq. (5) ($\lambda_{m,eff}$ and v_{eff}) and the determined ratio v_{eff}/v, which is based on numerical simulations. (a) using three different R_b values and an heat transfer rate of 50 W m^{-1}; (b) using four different q values and an thermal borehole resistance of 0.09 m K W^{-1}.

porous medium λ_m from 1.2 to 5.2 W m^{-1} K^{-1} and a Darcy velocity v interval from 0.01 to 3.5 m day^{-1} are performed and analyzed. Furthermore, the ratio v_{eff}/v is calculated for three different R_b values and four different extraction or injection rates, respectively (Fig. 6).

The determined ratio v_{eff}/v does not vary significantly for the three different R_b values, which is expected, because R_b is only related to the heat transfer inside the BHE. Thus, it is possible to exclude R_b from a TRT evaluation procedure and determine R_b separately. The focus of the TRT evaluation is on the heat transfer from the borehole wall to the subsurface (or vice versa). The ratio v_{eff}/v shows a clear linear correlation between the obtained Darcy velocity, v_{eff}, and the determined thermal conductivity of the porous medium, $\lambda_{m,eff}$. The wavering curve shape of the v_{eff}/v ratio arrays 0.9 and 1.0 (Fig. 6) are mainly caused by the decreasing influence of advective heat transport, resulting in a substantial uncertainty of the determined v_{eff} value. The determined ratio v_{eff}/v is even less influenced by the applied heat transfer rate. This is expected, because the heat transfer rate is simulated by the moving line source (Eq. (5)).

To transfer the results to an applicable correction term C, only the averages of v_{eff}/v for the three analyzed R_b values and four different extraction or injection rates are quantified, which are shown in Fig. 7. As explained previously, the determination of v_{eff}/v starts to become vague for low groundwater velocities. This inaccuracy

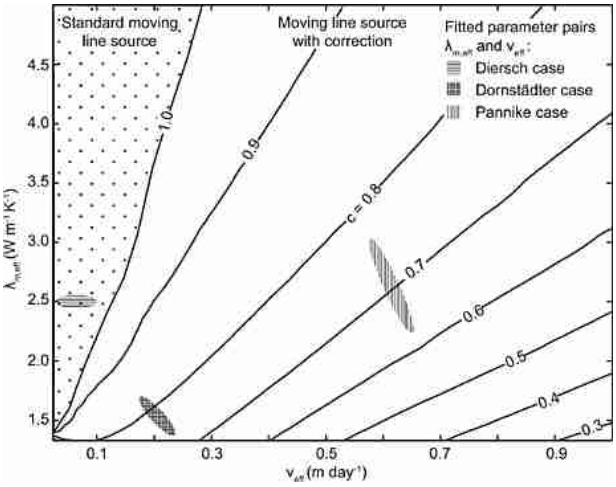

Fig. 7. Relation between the resulting parameters of the TRT evaluation based on Eq. (5) ($\lambda_{m,eff}$ and v_{eff}) and the determined correction term C. For the dotted parameter range of $\lambda_{m,eff}$ and v_{eff}, no correction is required, and for the white parameter range a correction of v_{eff} based on Eq. (10) is suggested. Parameter pairs ($\lambda_{m,eff}$ and v_{eff}) of the three studied test cases presented in Section 5 are highlighted.

also affects the determined C values. Thus, we defined a field of application ($C < 1$) in which the resulting Darcy velocity v_{eff} of the moving line source evaluation (Eq. (5)) should be corrected by C. Inside this area v_{eff} systematically underestimates v, and outside of this area (dotted range in Fig. 7) no correction of the obtained v_{eff} value is required.

4.2. Correction procedure

We suggest a three-step procedure to quantify both thermal (R_b, λ_m) and hydraulic (v) parameters from the TRT.

(1) Determine R_b by an external approach. In our study, we used the numerical results (Fig. 3).
(2) Estimate $\lambda_{m,eff}$ (=λ_m) and v_{eff} by fitting the moving line source (Eq. (5)) to the measured temperature time series.
(3) Obtain v^*_{eff} (= v) by correction of v_{eff} (Eq. (10)) with C taken from Fig. 7. For low v_{eff}, no correction is necessary ($C = 1$).

5. Application

To assess the proposed correction procedure for realistic GSHPs, three reported test cases are taken from the literature representing the field of application shown in Fig. 7 (Table 3). Based on the

Table 3
Thermal conductivities λ_m and λ_g, calculated thermal borehole resistances R_b, and Darcy velocities v from the three case studies for the application of the proposed correction procedure.

	Diersch case	Dornstädter case	Pannike case
Thermal conductivity of the grout, λ_g (W m^{-1} K^{-1})	2.3[a]	0.5[b]	0.8[b]
Thermal borehole resistance, R_b (m K W^{-1})	0.05[d]	0.14[d]	0.09[d]
Thermal conductivity of the porous medium, λ_m (W m^{-1} K^{-1})	2.5[a]	1.5[a]	2.7[a]
Darcy velocity, v (m day^{-1})	0.05[a]	0.25[a]	0.86[a]
Péclet number, Pe	0.05[c]	0.4[c]	0.8[c]

[a] Values from literature Diersch et al. (2010), Dornstädter et al. (2008) or Pannike et al. (2006), respectively.
[b] Values estimated.
[c] Values calculated based on the reported values and using Eq. (9).
[d] Values calculated based on Eq. (2) and the numerical result.

provided conditions, numerical TRT temperature time series are simulated and illustrated in Fig. 8. All other settings are listed in Tables 1 and 2. The generated temperature time series are evaluated by the proposed correction approach and the resulting parameter values are compared to the assigned input values to assess the procedure.

5.1. Diersch case

Diersch et al. (2010) simulated a shallow geothermal energy storage system installed in South-West Germany. The entire energy storage system consists of 80 BHEs, which are placed in a circular field with a radius of 15 m (Diersch et al., 2011). Each installed BHE is influenced by an underlying limestone aquifer with $\lambda_m = 2.4\,W\,m^{-1}\,K^{-1}$ and a maximum reported Darcy velocity of $v = 0.05\,m\,day^{-1}$. Based on both parameters an artificial temperature time series is generated by the numerical model and evaluated with the presented approach. This case study represents the conditions with lowest Darcy velocity and is dominated by conductive heat transport, which is also indicated by the small Péclet number ($Pe = 0.05$) (Fig. 9).

The results of the Diersch case TRT evaluation are shown in Fig. 8a. The competitive character of conductive and advective heat transport is indicated by a minor negative correlation. Still, the thermal conductivity focuses in a small range between 2.4 and $2.55\,W\,m^{-1}\,K^{-1}$. This only means a slight potential overestimation of the given value of $\lambda_m = 2.4\,W\,m^{-1}\,K^{-1}$. Conduction dominates the heat transfer ($Pe = 0.04$), and the small contribution by advection therefore may be misinterpreted as a higher impact from conduction. Under such conditions, however, extracting the role of advection is a challenging task. Even if feasible solutions of $\lambda_{m,eff}$ and v_{eff} very close to the real values are found, the range of possible v^*_{eff} results exceeds the predefined validity interval of ±10%. This confirms our expectations for the limited applicability of the presented approach for aquifers with low groundwater velocities. Obviously, even if λ_m can be estimated very well, more information can hardly be extracted from the TRT interpretation procedure. At most, it can be concluded that a very small Darcy velocity ($v < 0.1\,ms^{-1}$) is present.

5.2. Dornstädter case

Dornstädter et al. (2008) evaluated an enhanced TRT by a Péclet number analysis. The studied BHE is 57 m deep and is influenced by an aquifer with $\lambda_m = 1.5\,W\,m^{-1}\,K^{-1}$ and a maximum reported Darcy velocity of $v = 0.25\,m\,day^{-1}$. The aquifer ranges from 7 m to 14 m below ground level and is mainly built up of gravel. The hydraulic and thermal settings are used to generate an artificial TRT dataset, which is evaluated by the presented approach. From the selected case studies, the Dornstädter case represents the intermediate variant, with considerable but not extreme Darcy velocity. The calculated *Pe* indicates that the Dornstädter case is more influenced by advective heat transport than the Diersch case, but less

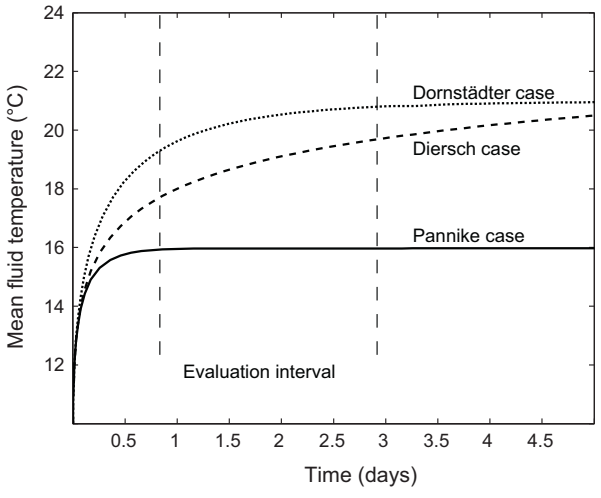

Fig. 8. Numerically generated temperature time series of the three evaluated test cases (Diersch case, Dornstädter case, Pannike case).

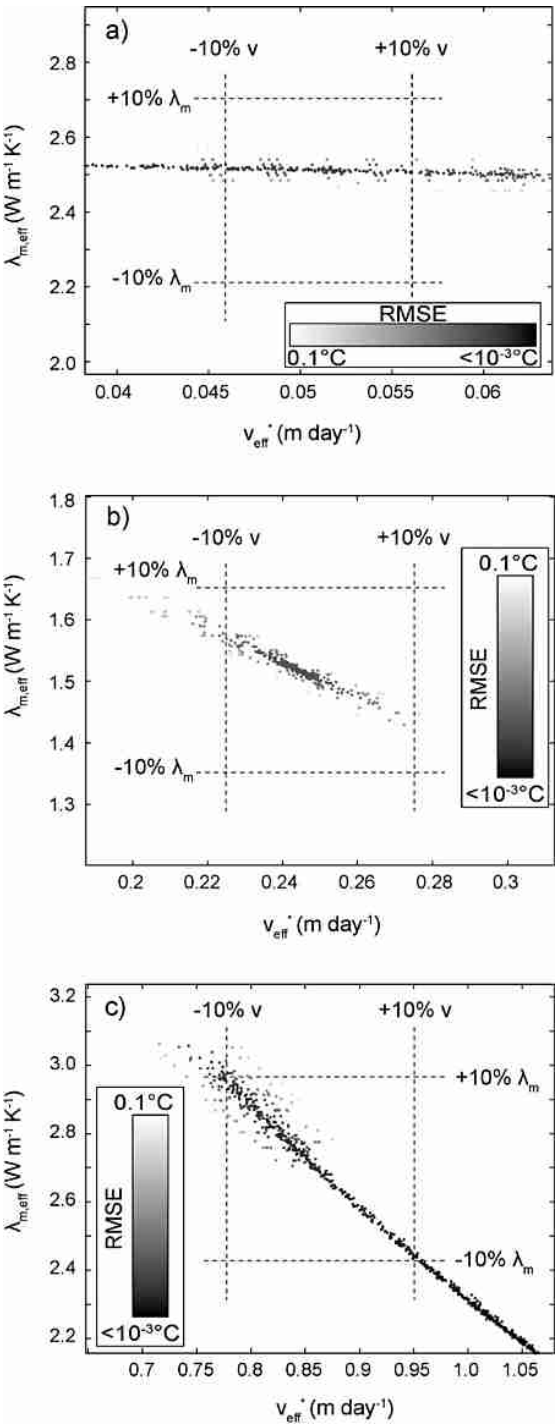

Fig. 9. Valid parameter pairs of $\lambda_{m,eff}$ and v^*_{eff} for an RMSE ≤ 0.1 °C. Dashed lines delineate the predefined tolerance window of ± 10% around the initial values listed in Table 3 for the different cases. (a) Diersch case; (b) Dornstädter case; (c) Pannike case.

than the following Pannike case. Nevertheless, in the Dornstädter case, conductive heat transport is more pronounced.

Again, the fitting procedure provides a nearly linear correlation of the possible solutions for $\lambda_{m,eff}$ and v^*_{eff}, which is presented in Fig. 8b. This reflects the similar effects of conduction and advection, although the higher contribution from advection yields a steeper trend, i.e., a more pronounced negative correlation. In contrast to the Diersch case, the estimated results for both parameters comply very well with the real values. Even if – for the given tolerance of the RMSE – numerous results are valid, the possible solution pairs only slightly exceed the ±10% boundary. We conclude that for conditions similar to this Dornstädter case ($Pe = 0.4$), the presented corrected moving line source procedure turns out to be very efficient.

5.3. Pannike case

Pannike et al. (2006) analyzed numerically the thermal plume caused by a BHE in several aquifers with varying hydraulic and thermal properties, which are typical of northern Germany. We extract the case with the highest Darcy velocity $v = 0.86\,\mathrm{m\,day^{-1}}$ and a thermal conductivity of the porous medium $\lambda_m = 2.7\,\mathrm{W\,m^{-1}\,K^{-1}}$. The conditions from the Pannike study are used to generate an artificial TRT dataset influenced by the highest Darcy velocity for testing the presented TRT evaluation approach. Based on the high Darcy velocity, the resulting Péclet number is $Pe = 0.8$, which indicates that heat is transported in comparable proportions by conduction and advection.

Similar to the previous cases, the results of the TRT evaluation show a negative linear correlation between λ_m and v^*_{eff} (Fig. 8c), which is further pronounced by the relatively high contribution from advective heat transport. Here, valid parameter values are nearly proportional. A relative change in v^*_{eff} is balanced by the same relative change in $\lambda_{m,eff}$. For the given RMSE threshold $\leq 0.1\,^{\circ}\mathrm{C}$, the parameters span a broad range, which not only meets but also exceeds the ±10% error window. For example, for the given $v = 0.86\,\mathrm{m\,day^{-1}}$, v^*_{eff} values are found to be between 0.6 and 1.1. The true thermal conductivity $\lambda_m = 2.7\,\mathrm{W\,m^{-1}\,K^{-1}}$ is equally over- and underestimated with values between $\lambda_{m,eff} = 2.0$ and $3.5\,\mathrm{W\,m^{-1}\,K^{-1}}$. In practice, this means that by the procedure at least a considerable influence of advection can be detected and also a plausible range can be determined. In the specific Pannike case, close-to-reality solutions can be found by taking the (visual) mean (or statistical median) from Fig. 8c, but in practice this might be biased by measurement errors or other sources of noise. Often, it is possible to further confine reasonable ranges of the expected thermal conductivity based on rock or sediment facies. For example, Woodside and Messmer (1961) and Popov et al. (1999) presented several methods to estimate ranges of thermal conductivity for unconsolidated materials, which could be used as constraints to improve the estimation of the prevailing Darcy velocity.

Finally, we could demonstrate for all studied test cases that the resulting parameters of the presented evaluation procedure are representative properties of the subsurface. The Diersch case, which represents a low-advection case, shows that no further correction is necessary and the evaluation is not sensitive for the estimation of the Darcy velocity within the assigned relative error range. The Dornstädter case, which is a medium-advection case, shows that the proposed correction approach results in acceptable estimates for $\lambda_{m,eff}$ and v^*_{eff}. Although the R_b value of the simulated BHE exceeds the used R_b range for determination of the correction term C, the accuracy of the estimated parameters is very high. This is evidence that the field of application might exceed the considered R_b range for the determination of C (Fig. 6). The Pannike case, which represents the highly advective case, reveals the non-uniqueness of the inverse problem, which prevents an unequivocal estimation of $\lambda_{m,eff}$ and v^*_{eff}. However, the accuracy can be efficiently improved, if the representative thermal conductivity of the porous medium can be constrained. Nevertheless, four main challenges still remain: First, the effect of subsurface heterogeneity has to be analyzed in more detail and in particular, if the examined BHE is only partially groundwater-influenced. Secondly, the role of different evaluation times should be further analyzed. Thirdly, the heat capacity ratio between the groundwater and the solid might also influence the result of the evaluation. Finally, the validation of the presented evaluation procedure in the field is necessary.

6. Conclusion

In this study, an innovative analytical approach to the evaluation of groundwater-influenced TRTs is introduced and applied using three different case studies from the literature. The approach includes a correction procedure to mitigate the error that is caused by the hydraulic parameter contrast between the grouting material and the subsurface. The derived procedure is verified by high-resolution numerical simulations.

With the results of the numerical simulations we demonstrate that for a wide range of groundwater-influenced TRTs, the Darcy velocity cannot be determined simply by the moving line source theory. Hence, we derived a correction procedure to overcome the limitations of a line-shaped heat source in a homogeneous flow field describing a BHE. The analyses of three TRT test cases are performed to assess the simultaneous determination of $\lambda_{m,eff}$ and v^*_{eff}. Due to the competitive character of conductive and advective heat transport around a BHE, the assessment of all three test cases results in an array of possible solutions and not only in a single valid parameter pair. However, all solution sets contain possible "true" parameter combinations and $\lambda_{m,eff}$ and v^*_{eff} always exhibit a negative correlation.

For conduction-dominated cases ($Pe < 0.1$), the result obtained by the moving line source theory cannot be further improved by the correction approach. The evaluation procedure results in a wide range of valid v^*_{eff} values, which exceeds the given error tolerance interval of ±10%. In contrast, the resulting thermal conductivity value $\lambda_{m,eff}$ matches rather precisely the value assigned in the numerical simulation. For the moderate test case, with a Pe number in the range of 0.1–0.8, an excellent distinction between advective and conductive contribution could be achieved. Almost all possible parameter pairs ($\lambda_{m,eff}$ and v^*_{eff}) are within the ±10% error interval. The results of the test case with the highest Darcy velocity ($v = 0.9\,\mathrm{m\,day^{-1}}$) show that even for a small error tolerance (RMSE < 0.1), a broad range of parameter pairs of λ_{eff} and v^*_{eff} provide suitable results. However, based on the significant negative correlation between $\lambda_{m,eff}$ and v^*_{eff}, the latter can be more precisely determined, if the representative thermal conductivity of the porous medium is separately estimated. Thus, for high Pe numbers ($Pe \geq 0.8$), the TRT could also be used as a hydraulic test method.

Acknowledgements

We would like to thank Jozsef Hecht-Méndez, Hagen Steger, Nelson Molina-Giraldo and two anonymous reviewers for their fruitful comments. Furthermore, the support of Heidi Knierim in preparing the manuscript is also gratefully acknowledged.

References

Bandos, T.V., Montero, Á., Fernández de Córdoba, P., Urchueguía, J.F., 2011. Improving parameter estimates obtained from thermal response tests: effect of ambient air temperature variations. Geothermics 40 (2), 136–143.

Bandos, T.V., Montero, Á., Fernández, E., Santander, J.L.G., Isidro, J.M., Pérez, J., Córdoba, P.J.F.d., Urchueguía, J.F., 2009. Finite line-source model for borehole heat exchangers: effect of vertical temperature variations. Geothermics 38 (2), 263–270.

Barcenilla, J.R., Nutter, D.W., Couvillion, R.J., 2005. Effective thermal conductivity for single-bore vertical heat exchangers with groundwater flow. ASHRAE Transactions 111 (2), 258–263.

Bauer, D., Heidemann, W., Muller-Steinhagen, H., Diersch, H.J.G., 2011. Thermal resistance and capacity models for borehole heat exchangers. International Journal of Energy Research 35 (4), 312–320.

Beier, R.A., Smith, M.D., Spitler, J.D., 2011. Reference data sets for vertical borehole ground heat exchanger models and thermal response test analysis. Geothermics 40 (1), 79–85.

Bozdag, S., Turgut, B., Paksoy, H., Dikici, D., Mazman, M., Evliya, H., 2008. Ground water level influence on thermal response test in Adana, Turkey. International Journal of Energy Research 32 (7), 629–633.

Carslaw, H.S., Jaeger, J.C., 1959. Conduction of Heat in Solids. Clarendon Press, Oxford, p. 510.

Chiasson, A., O'Connell, A., 2011. New analytical solution for sizing vertical borehole ground heat exchangers in environments with significant groundwater flow: parameter estimation from thermal response test data. HVAC&R Research 17 (6), 1000–1011.

Chiasson, A.C., Rees, S.J., Spitler, J.D., 2000. A preliminary assessment of the effects of ground-water flow on closed-loop ground-source heat pump systems. ASHRAE Transactions 106 (1), 380–393.

Clausen, H., 2008. Durchführung von Simulationsrechnungen zum Einfluss verschiedener Randbedingungen auf die thermische Leistungsfähigkeit von Erdwärmesonden, Diploma thesis, Universität Stuttgart.

Diersch, H., Bauer, D., Heidemann, W., Rühaak, W., Schätzl, P., 2010. Finite element formulation for borehole heat exchangers in modeling geothermal heating systems by FEFLOW. WASY Software FEFLOW White Paper 5, 5–96.

Diersch, H.J.G., 2006. FEFLOW 5.3 User's Manual. WASY GmbH, Berlin.

Diersch, H.J.G., Bauer, D., Heidemann, W., Rühaak, W., Schätzl, P., 2011. Finite element modeling of borehole heat exchanger systems: Part 2. Numerical simulation. Computers & Geosciences 37 (8), 1136–1147.

Domenico, P.A., Palciauskas, V.V., 1973. Theoretical analysis of forced convective heat transfer in regional ground-water flow. Geological Society of America Bulletin 84 (12), 3803–3814.

Dornstädter, J., Heidinger, P., Heinemann-Glutsch, B., 2008. Erfahrungen aus der Praxis mit dem Enhanced Geothermal Response Test (EGRT). In: Der Geothermiekongress 2008, Karlsruhe, pp. 271–279.

Fujii, H., Okubo, H., Nishi, K., Itoi, R., Ohyama, K., Shibata, K., 2009. An improved thermal response test for U-tube ground heat exchanger based on optical fiber thermometers. Geothermics 38 (4), 399–406.

Gauthier, C., Lacroix, M., Bernier, H., 1997. Numerical simulation of soil heat exchanger-storage systems for greenhouses. Solar Energy 60 (6), 333–346.

Gehlin, S., 2002, Thermal response test method development and evaluation, Doctoral thesis, Luleå University of Technology.

Gehlin, S.E.A., Hellström, G., Nordell, B., 2003. The influence of the thermosiphon effect on the thermal response test. Renewable Energy 28 (14), 2239–2254.

Gustafsson, A.M., Gehlin, S., 2008. Influence of natural convection in water-filled boreholes for GCHP. ASHRAE Transactions 114 (1), 416–423.

Gustafsson, A.M., Westerlund, L., 2010. Multi-injection rate thermal response test in groundwater filled borehole heat exchanger. Renewable Energy 35 (5), 1061–1070.

Gustafsson, A.M., Westerlund, L., 2011. Heat extraction thermal response test in groundwater-filled borehole heat exchanger – investigation of the borehole thermal resistance. Renewable Energy 36 (9), 2388–2394.

Hähnlein, S., Molina-Giraldo, N., Blum, P., Bayer, P., Grathwohl, P., 2010. Ausbreitung von Kältefahnen im Grundwasser bei Erdwärmesonden. (Cold plumes in groundwater for ground source heat pump systems). Grundwasser 15 (2), 123–133.

Hecht-Méndez, J., Molina-Giraldo, N., Blum, P., Bayer, P., 2010. Evaluating MT3DMS for heat transport simulation of closed geothermal systems. Ground Water 48 (5), 741–756.

Hellström, G., 1991, Ground heat storage, thermal analyses of duct storage systems, Doctoral thesis, Luleå University of Technology.

Hellström, G., Sanner, B., 2000, Earth Energy Designer-EED. User manual. Blocon, Lund.

Herrmann, J., 2008, Ingenieurgeologische Untersuchungen zur Hinterfüllung von Geothermie-Bohrungen mit Erdwärmesonden, Doctoral thesis, Fridericiana University of Karlsruhe.

Katsura, T., Nagano, K., Takeda, S., Shimakura, K., 2006. Heat transfer experiment in the ground with ground water advection. In: The IEA 10th Energy Conservation Thermal Energy Storage Conference, New Jersey, USA.

Lagarias, J.C., Reeds, J.A., Wright, M.H., Wright, P.E., 1998. Convergence properties of the Nelder–Mead simplex method in low dimensions. SIAM Journal on Optimization 9 (1), 112–147.

Lamarche, L., Kajl, S., Beauchamp, B., 2010. A review of methods to evaluate borehole thermal resistances in geothermal heat-pump systems. Geothermics 39 (2), 187–200.

Maier, U., DeBiase, C., Baeder-Bederski, O., Bayer, P., 2009. Calibration of hydraulic parameters for large-scale vertical flow constructed wetlands. Journal of Hydrology 369 (3–4), 260–273.

Marcotte, D., Pasquier, P., 2008. On the estimation of thermal resistance in borehole thermal conductivity test. Renewable Energy 33 (11), 2407–2415.

Metzger, T., Didierjean, S., Maillet, D., 2004. Optimal experimental estimation of thermal dispersion coefficients in porous media. International Journal of Heat and Mass Transfer 47 (14–16), 3341–3353.

Molina-Giraldo, N., Bayer, P., Blum, P., 2011. Evaluating the influence of thermal dispersion on temperature plumes from geothermal systems using analytical solutions. International Journal of Thermal Sciences 50 (7), 1223–1231.

Morgensen, P., 1983. Fluid to duct wall heat transfer in duct system heat storage. In: International Conference on Surface Heat Storage in Theory and Practice, Stockholm, Sweden.

Niekamp, A., Unklesbay, K., Unklesbay, N., Ellersieck, M., 1984. Thermal-properties of bentonite–water dispersions used for modeling foods. Journal of Food Science 49 (1), 28–31.

Palmer, C.D., Blowes, D.W., Frind, E.O., Molson, J.W., 1992. Thermal-energy storage in an unconfined aquifer.1. Field injection experiment. Water Resources Research 28 (10), 2845–2856.

Pannike, S., Kölling, M., Panteleit, B., Reichling, J., Scheps, V., Schulz, H.D., 2006. Auswirkung hydrogeologischer Kenngrößen auf die Kältefahnen von Erdwärmesondenanlagen in Lockersedimenten. Grundwasser 11, 6–18.

Popov, Y.A., Pribnow, D.F.C., Sass, J.H., Williams, C.F., Burkhardt, H., 1999. Characterization of rock thermal conductivity by high-resolution optical scanning. Geothermics 28 (2), 253–276.

Raymond, J., Therrien, R., Gosselin, L., 2011a. Borehole temperature evolution during thermal response tests. Geothermics 40 (1), 69–78.

Raymond, J., Therrien, R., Gosselin, L., Lefebvre, R., 2011b. Numerical analysis of thermal response tests with a groundwater flow and heat transfer model. Renewable Energy 36 (1), 315–324.

Raymond, J., Therrien, R., Gosselin, L., Lefebvre, R., 2011c. A review of thermal response test analysis using pumping test concepts. Ground Water, http://dx.doi.org/10.1111/j.1745-6584.2010.00791.x

Roth, P., Georgiev, A., Busso, A., Barraza, E., 2004. First in situ determination of ground and borehole thermal properties in Latin America. Renewable Energy 29 (12), 1947–1963.

Rybach, L., Eugster, W.J., 2010. Sustainability aspects of geothermal heat pump operation, with experience from Switzerland. Geothermics 39 (4), 365–369.

Sanner, B., Hellström, G., Spitler, J., Gehlin, S., 2005. Thermal response test – current status and world wide application. In: World Geothermal Congress, Antalya, Turkey, pp. 1436–1445.

Sanner, B., Karytsas, C., Mendrinos, D., Rybach, L., 2003. Current status of ground source heat pumps and underground thermal energy storage in Europe. Geothermics 32 (4–6), 579–588.

Signorelli, S., Bassetti, S., Pahud, D., Kohl, T., 2007. Numerical evaluation of thermal response tests. Geothermics 36 (2), 141–166.

Sutton, M.G., Nutter, D.W., Couvillion, R.J., 2002. A ground resistance for vertical bore heat exchangers with groundwater flow. ASME Journal of Energy Resources Technology 125, 183–189.

Taniguchi, M., Uemura, T., 2005. Effects of urbanization and groundwater flow on the subsurface temperature in Osaka, Japan. Physics of the Earth and Planetary Interiors 152 (4), 305–313.

Wagner, R., Rohner, E., 2008. Improvements of thermal response tests for geothermal heat pumps. In: IEA Heat Pump Conference, Zürich, Switzerland.

Wagner, V., Bayer, P., Kübert, M., Blum, P., 2012. Numerical sensitivity study of thermal response tests. Renewable Energy 41 (0), 245–253.

Witte, H.J.L., 2001. Geothermal response test with heat extraction and heat injection: examples of application in research and design of geothermal ground heat exchangers. In: Europäischer Workshop über Geothermische Response Tests, Lausanne, Switzerland.

Witte, H.J.L., Gelder, G.V., 2006. Geothermal response tests using controlled multi-power level heating and cooling pulses (MPL-HCP): quantifying ground water effects on heat transport around a borehole heat exchanger. In: Proceedings of the Tenth International Conference on Thermal Energy Storage, New Jersey, USA.

Witte, H.J.L., van Gelder, G.J., Spitler, J.D., 2002. In-situ measurements of ground thermal conductivity: the Dutch perspective. ASHRAE Transactions Research 108 (1), 263–272.

Woodside, W., Messmer, J.H., 1961. Thermal conductivity of porous media. I. Unconsolidated sands. Journal of Applied Physics 32 (9), 1688–1699.

Zhu, K., Blum, P., Ferguson, G., Balke, K.D., Bayer, P., 2011. The geothermal potential of urban heat islands. Environmental Research Letters 5 (044002), 1–6.